MHD Simulation of Energy Transfer From the Solar Wind Into the Magnetosphere

M. Palmroth[1], T. I. Pulkkinen[1], and P. Janhunen[1]

[1]Finnish Meteorological Institute, Geophysical Research Division
P.O.Box 503, 00101 Helsinki, Finland;
minna.palmroth@fmi.fi

Abstract. We use a 3D global magnetohydrodynamic (MHD) simulation code to examine the energy flow from the solar wind into the magnetosphere. We simulate two time periods: a major magnetospheric storm on April 6-7, 2000, and a substorm on August 15, 2001. During the storm event the energy input into the magnetosphere was highly enhanced, but during the substorm event the energy input was more typical. For the energy transfer calculation, a method for identifying the magnetopause surface from the simulation is developed. We calculate the total energy flux component normal to the magnetopause surface, thus giving the energy flux transferred from the solar wind into the magnetosphere. With this method we identify the locations on the magnetopause surface where significant energy transfer takes place. We also compare the time evolution of the total transferred energy to the time evolution of the empirical ε parameter calculated from the solar wind parameters.

1. Introduction

One of the fundamental questions in magnetospheric physics is trying to quantify the global energy transfer process between the solar wind and the magnetosphere. Observationally, this task would need a massive network of satellites, and therefore the energy transfer process has been investigated only locally or by using various coupling parameters, of which the ε parameter [*Akasofu*, 1981] is the most widely used. However, the coupling parameters, where a point measurement in the solar wind is correlated with various magnetospheric activity parameters, can only give a crude estimation of the transferred energy, and they tell nothing about where the energy transfer takes place at the magnetopause.

The global MHD simulations may hold a potential answer to the global energy transfer process, within the limitations of the MHD approach to describe the dynamical solar wind – magnetosphere – ionosphere system. In this study we examine energy flow from the solar wind through the magnetopause during two events: a major magnetospheric storm and a substorm. Our approach is to first find the magnetopause from the simulation results and then calculate the total energy flux component normal to the magnetopause. This paper is an extension to *Palmroth et al.* [2002], where the method is introduced in detail. The purpose of this paper is to compare the energy transfer processes during strongly driven period (storm) and more typical conditions (substorm).

2. Model

GUMICS-4 is a global magnetospheric MHD simulation code, which solves MHD equations in fully conservative form in the magnetosphere and solar wind, and electrostatic current continuity equations in the ionospheric domain [*Janhunen*, 1996]. The ionosphere is solved in a three-dimensional grid with 20 nonuniform height levels. The ionospheric potential is a boundary condition for the MHD equations at the edge of the magnetospheric domain, which is a spherical shell with radius of 3.7 R_E. GUMICS-4 uses an automatically adaptive Cartesian octogrid in the magnetospheric domain. In the ionospheric domain the triangular grid is fixed in

time, although refined in the auroral oval region. The present simulation results were carried out in a code setup similar to the one used in *Palmroth et al.* [2001].

In this paper we introduce results from two MHD simulations; a storm period on April 6-7, 2000 (for description of the storm observations, see *Huttunen et al.*, [2002]), and a substorm period on August 15, 2001. A period of 17 hours was simulated starting from 14 UT on April 6, 2000, whereas 6 hours was simulated starting from 2 UT on August 15, 2001. Wind and IMP-8 satellites were used as the upstream boundary condition for the two simulations, respectively. The densest grid sizes were 0.5 R_E and 0.25 R_E for the April 2000 and the August 2001 runs, respectively.

3. Magnetopause Surface Identification from MHD Simulation

Evaluation of the solar wind energy transfer to the magnetosphere requires a definition of an appropriate surface, the magnetopause. Here the magnetopause is searched automatically from the simulation: At the beginning of the magnetopause search, a set of 10,000 streamlines at 15 R_E is followed in 0.5 R_E steps to the antisunward direction. For each 0.5 R_E step the algorithm searches for a void of streamlines around the X_{GSE} axis. Finding such a void of streamlines indicates that the streamlines have started to bend around the magnetosphere. The algorithm finds the inner boundary of the void, which defines the magnetopause in the $Y_{GSE}Z_{GSE}$ plane. For more information of the method, see *Palmroth et al*. [2002]. Note that although the subsolar position is a point on the X_{GSE} axis, the magnetosphere itself needs not to be aligned with the X_{GSE} axis, and the magnetospheric boundary in the $Y_{GSE}Z_{GSE}$ plane is not necessarily circular. Figure 1 shows an example of the surface generated from the GUMICS files. The surface is from April 2000 run, just after the interplanetary magnetic cloud hit the magnetosphere.

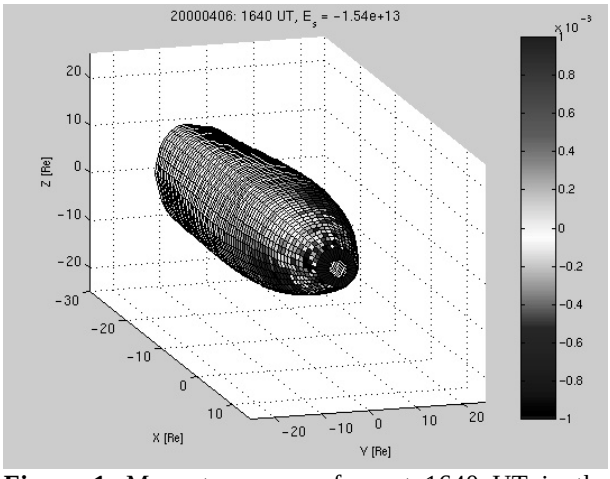

Figure 1. Magnetopause surface at 1640 UT in the April 2000 run. Gray shades show the total energy flux component normal to the surface.

4. Energy Flow Through Magnetopause in MHD Simulation

When the surface coordinates are known, the energy flow across each quadrangular surface element defined by the surface grid can be computed. We calculate the area of the surface element *dA* and the surface normal unit vector $\mathbf{n}_q$. The energy flux dE_q across the quadrangular surface element is

$$dE_q = dA\ \mathbf{K}\cdot\mathbf{n}_q. \qquad (1)$$

K is the total energy flux density (W/m^2), defined as

$$\mathbf{K} = \left(U+P-\frac{B^2}{2\mu_0}\right)\mathbf{v} + \frac{1}{\mu_0}\mathbf{E}\times\mathbf{B}, \qquad (2)$$

where U is the total energy density

$$U = \frac{P}{\gamma-1} + \frac{1}{2}\rho\mathbf{v}^2 + \frac{B^2}{2\mu_0}, \qquad (3)$$

where P is the pressure, ρ density, **v** velocity, **B** magnetic field, and $\mathbf{E} = \mathbf{B}\times\mathbf{v}$ is the electric field. The total energy flux density **K** is interpolated from the GUMICS-4 MHD simulation at the center of each surface element. The total energy flux through the surface is then the sum of the energy fluxes of each surface element,

$$E_S = \int dE_q \,. \qquad (3)$$

Figure 1 shows the total energy flux normal to the magnetopause surface at the SSC as gray shades in the April 2000 storm run.

5. Results: April 6-7, 2000

Figure 2 shows the total integrated energy flux E_s through the surface in the April 2000 storm simulation. Also plotted is the ε parameter calculated from the solar wind parameters. The two curves are remarkably similar during the storm main phase (~18-24 UT) with the energy through the surface in the simulation being about four times larger than the ε parameter. The differences appear during the SSC and the recovery phase. In the SSC, ε increases only to about half of its maximum during the storm period, whereas E_s increases to a level also typical of the main phase. Furthermore, during the recovery phase ε decreases close to zero, while E_s still shows significant energy input through the surface. We also calculated the effect caused by the surface motion during the storm period. The effect was largest during the SSC and the recovery phase, when it was about 2% of E_s. During the main phase the surface motion effect was below 1% of E_s.

Figure 3 shows the total energy flux through the surface integrated over surface slices. Figures 3a-3d are the total energy fluxes over surface slices $-30 \le X_{GSE} \le -20$ R_E, $-20 < X_{GSE} \le -10$ R_E, $-10 < X_{GSE} \le 0$ R_E, and $X_{GSE} > 0$ R_E, respectively, Figure 3e is the IMF B_z component. In Figures 3c and 3d ε is also plotted for reference (gray). The following facts are readily seen in Figure 3. 1) Most of the energy transferring from the solar wind comes through the surface sunward of the distance of -10 R_E. 2) Surface slide $-10 < X_{GSE} \le 0$ R_E seems to contribute the most in the energy transfer, although one must remember that the dayside slide is much smaller in area than the other slices, since the storm pushes the subsolar magnetopause nearer to the Earth than is usual. 3) The dayside slice contributes uniformly during the storm period: no apparent division into main and recovery phases can be done, as is the case for ε.

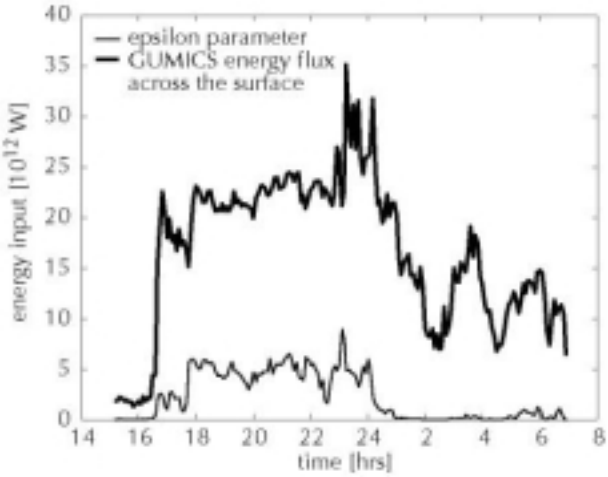

Figure 2. (Thick line) Total integrated energy flux through each generated surface in the April 2000 storm simulation. (Thin line) ε parameter calculated from the solar wind parameters.

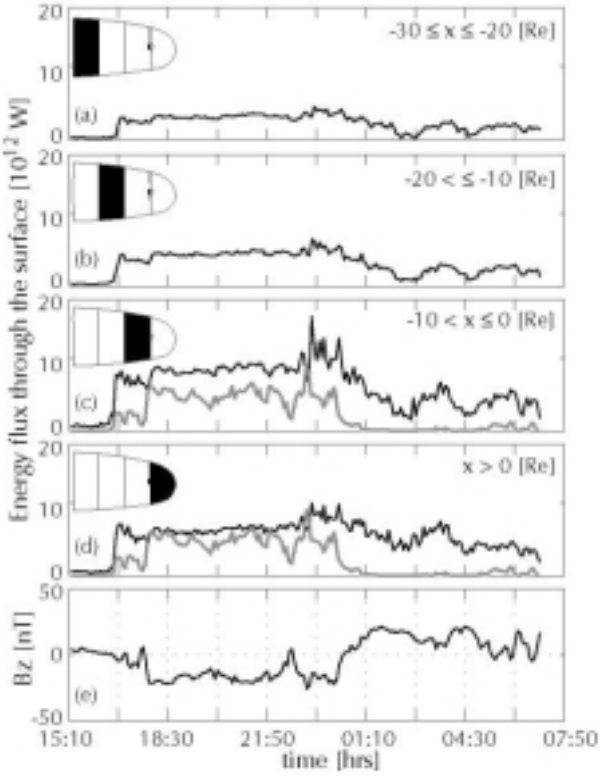

Figure 3. Total energy integrated over surface slices, i.e., the X_{GSE} –distribution of the total energy flux. Bottom panel shows the IMF B_z component.

Figure 4 shows the azimuthal distribution of the total transferred energy in the April 2000 storm simulation. Now the energy flux is integrated over

the azimuth angle; all X_{GSE} values are present in the azimuthal energy distribution.

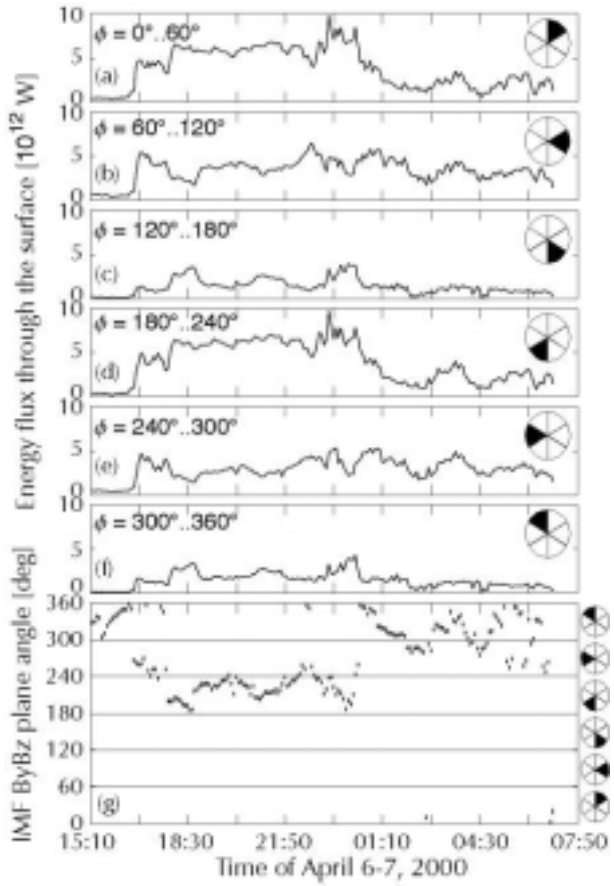

Figure 4. Azimuthal energy distribution in the April 2000 simulation. Bottom panel gives the IMF clock angle.

Figure 4a-4f give the transferred energy in sectors 0°…60°, 60°…120°, 120°…180°, 180°…240°, 240°…300°, 300°…360°, respectively, and Figure 4g gives the angle $\theta = \text{atan}(B_y/B_z)$, i.e., the IMF clock angle. The following facts are observable in Figure 4. 1) During the SSC (southward IMF), the IMF clock angle resides in sector 240°…300°, and most of the energy comes through that sector and also the sector antiparallel to it (sector 60°…120°). 2) During the main phase (southward IMF), the IMF clock angle is predominantly in sector 180°…240°, and most of the energy is transferred in that sector and also the sector antiparallel to it (sector 0°…60°). 3) During the SSC and main phases, the least amount of energy is transferred in the sectors perpendicular to the IMF clock angle plane. 4) During the recovery phase (northward IMF), the IMF clock angle fluctuates, but is predominantly in the sector 300°…360°. However, most of the energy is transferred in the low-latitude equatorial sectors.

6. Results: August 15, 2001

The top panel of Figure 5 shows the total transferred energy E_s during the substorm that occurred on August 15, 2001. Also plotted is the ε parameter scaled by a factor of 15. Bottom panel of Figure 5 shows the IMF B_z component. Figure 5 shows that ε starts to increase, when IMF B_z decreases below 2 nT. The ε maximum occurs at the same time with the IMF B_Z minimum, and with decreasing negative IMF B_z also ε decreases. The total transferred energy E_s in the simulation starts to increase when the IMF turns southward, and remains enhanced the whole time the IMF is southward. The decreasing phase starts only when the IMF turns northward, indicating that the peaks in ε and E_s are separated in time with the E_s peak occurring about half an hour later than the ε peak.

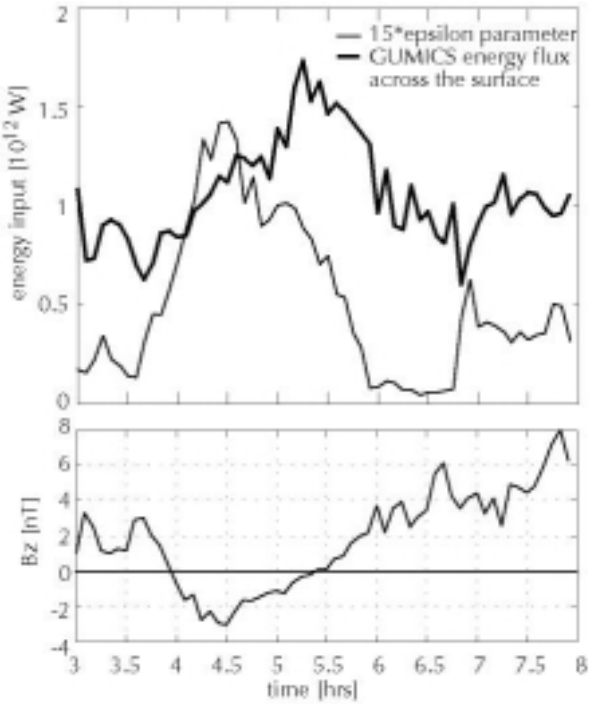

Figure 5. (Top) The total transferred energy during the August 15, 2001, substorm simulation, and the ε parameter scaled 15 times larger. (Bottom) IMF B_z.

Figure 6 shows the X_{GSE} distribution of the transferred energy during the August 15, 2001,

substorm simulation. The format of the figure is the same as in Figure 3. Again, most of the energy appears to come through the surface sunward of the distance −10 R_E. The mostly contributing slice is the $-10<X_{GSE}\leq 0$ R_E slice. Again, the dayside slice contributes uniformly throughout the substorm period.

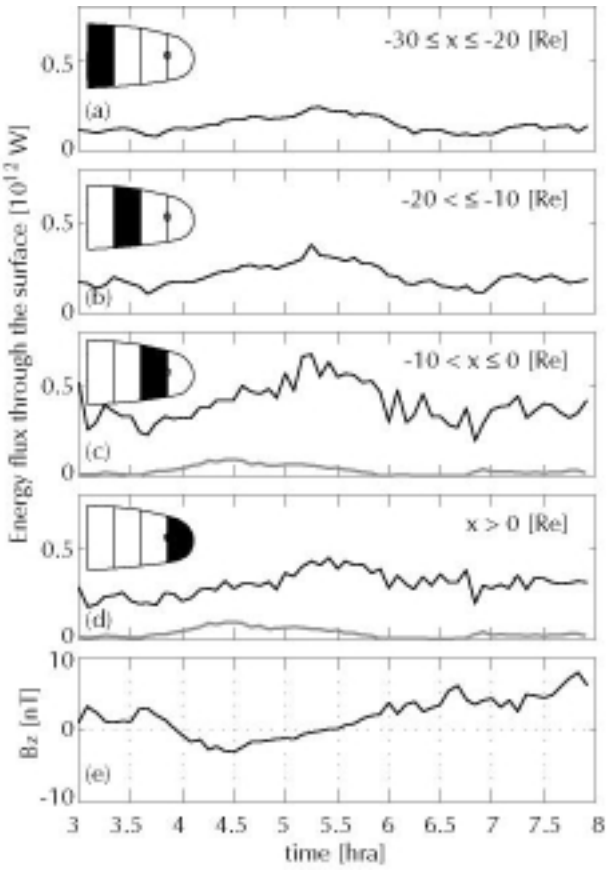

Figure 6. The total transferred energy distribution in the X_{GSE} axis. The format of the figure is the same as in Figure 3.

Figure 7 shows the azimuthal distribution of energy transferred in the August 15, 2001, simulation. The format of the figure is the same as in Figure 4. Before the IMF B_z turns southward and the substorm sequence begins, the IMF clock angle is in the sector 60°…120°. The mostly contributing sectors before the substorm onset are however the sectors 120°…180° and 300°…360°. During the southward IMF B_z period, the IMF clock angle rotates to the sector 120°…180°. Similarly as in the storm simulation, most of the energy transfers in that sector, and also the sector antiparallel to it (sector 300°…360°). When the IMF turns northward again, the IMF clock angle is about 60°, but most of the energy still comes from the sectors 120°…180° and 300°…360°. Also equatorial low-latitude sectors increase their contribution at the end of the simulated period. Very little energy comes through the sectors 0°…60° and 180°…240° during the simulated time.

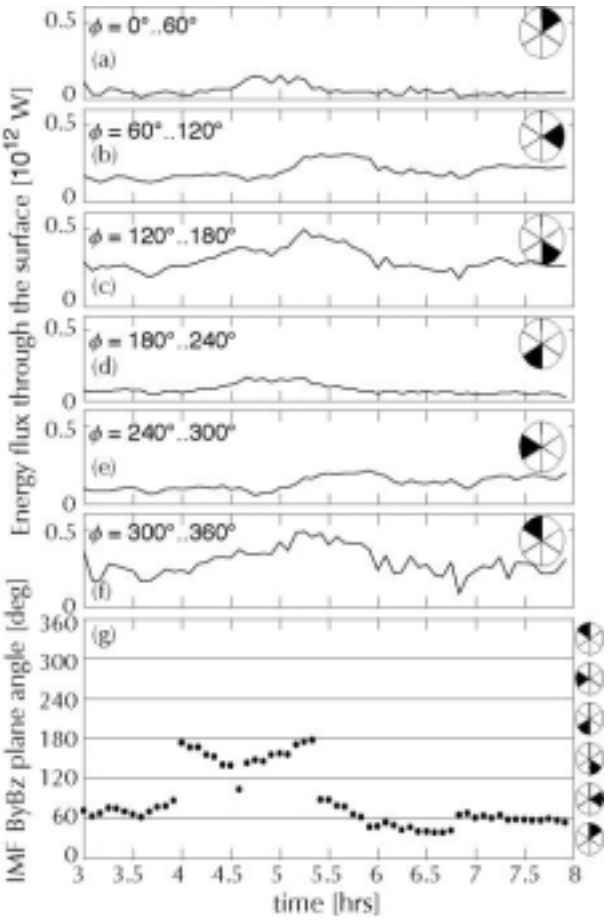

Figure 7. The azimuthal energy distribution during the August 15, 2001, substorm simulation. The format of the figure is the same as in Figure 4.

7. Summary and Conclusion

The purpose of this study was to investigate the ability of a global MHD model in quantifying the global energy transfer process between the solar wind and the magnetosphere. We developed a method for calculating the total energy flux through the magnetopause surface. With this method the locations on the magnetopause surface where the energy transfer takes place can be seen for the first time. To our knowledge, this is the first

time this kind of task has been carried out. Previously, *Papadopoulos et al.* [1999] carried out an investigation where Poynting flux flow lines were mapped in a global MHD simulation. However, since the amount of Poynting flux depends on the initial surface, we chose to use the conservative total energy flux.

Our simulation results show that during southward IMF the energy transfer occurs mostly sunward of X_{GSE} = -10 R_E. During southward IMF the dayside magnetopause is open due to reconnection [e.g., *Luhmann et al*., 1984]. Once the field line has been merged with the solar wind field line, it stays open until it reaches the tail reconnection region. Therefore, energy may enter freely along the open field line sunward of the tail reconnection region.

During southward IMF, we found that energy is transferred in relatively narrow sectors parallel and antiparallel to the IMF clock angle. The sectors perpendicular to the plane of the IMF clock angle show weakest energy transfer during southward IMF. We suggest that Poynting flux focusing [*Koskinen and Tanskanen*, 2002] controls the energy transfer sectors during southward IMF, because the Poynting flux focuses toward the magnetopause in the plane of the IMF clock angle. Otherwise, if reconnection was the only factor in the energy transfer locations, we would assume an even azimuthal energy transfer distribution.

During northward IMF the Poynting flux focusing does not seem to have a role in the energy transfer process. On the contrary, if one looks at Figure 2 of *Luhmann et al*. [1984], there seems to be a linkage between the reconnection regions during northward IMF and the energy transfer locations in our two simulation runs. However, this observation needs to be further investigated.

Overall, our results show that the shapes of the total energy flux through the magnetopause surface and the ε parameter agree sufficiently well during southward IMF. Since the ε represents the energy dissipated into the magnetosphere, it is not strictly legal to correlate our E_s and ε, because E_s is only the energy transferred through the surface, not entirely dissipated into the magnetosphere. Nonetheless, their interrelation needs to be further investigated.

Acknowledgments

The work of MP and PJ was supported by the MaDaMe –program of the Academy of Finland

References

Akasofu, S.-I., Energy coupling between the solar wind and the magnetosphere, *Space Sci. Rev*. **28**, 121-190, 1981.

Janhunen P., GUMICS-3 - A global ionosphere magnetosphere coupling simulation with high ionospheric resolution, in Proc. Environmental Modelling for Space-Based Applications, Sept. 18-20 1996 (ESTEC, The Netherlands, ESA SP-392, 1996).

Huttunen, K. E. J., H. E. J. Koskinen, T. I. Pulkkinen, A. Pulkkinen, M. Palmroth, and H. Singer, April 2000 magnetic storm: Solar wind driver and magnetospheric response, *J. Geophys. Res*., in press, 2002.

Koskinen, H. E. J., and E. I. Tanskanen, Magnetospheric energy budget and the epsilon parameter, submitted to the *J. Geophys. Res*., 2002.

Luhmann, J. G., R. J. Walker, C. T. Russell, N. U. Crooker, J. R. Spreiter, and S. S. Stahara, Patterns of potential magnetic field merging sites on the dayside magnetopause, *J. Geophys. Res.*, **89**, 1739-1742, 1984.

Palmroth, M., P. Janhunen, T. I. Pulkkinen, and W. K. Peterson, Cusp and magnetopause locations in global MHD simulation, J. Geophys. Res., 106, 29,435, 2001.

Palmroth, M., T. I. Pulkkinen, P. Janhunen, and C.-C. Wu, Stormtime energy transfer in global MHD simulation, submitted to the *J. Geophys. Res*., 2002.

Papadopoulos, K., C. Goodrich, M. WIltberger, R. Lopez, and J. G. Lyon, The physics of substorms as revealed by the ISTP, *Phys. Chem. Earth* (c), **24**, 189-202, 1999.